



## ORIGINAL ARTICLE

# Calixarene coated gold nanoparticles as a novel therapeutic agent

Sadia Khalid\*, Samina Parveen, Muhammad Raza Shah, Sana Rahim, Shakil Ahmed, Muhammad Imran Malik

International Center for Chemical and Biological Sciences, University of Karachi, Karachi 75270, Pakistan

Received 3 January 2019; accepted 25 April 2019

Available online 4 May 2019

## KEYWORDS

Gold nanoparticles;  
S. aureus;  
E. coli;  
Antibacterial mechanism;  
Phytotoxicity;  
Cytotoxicity and atomic force microscopy

**Abstract** In the current study, gold nanoparticles (*AuC6NPs* and *AuC8NPs*) were prepared through sodium borohydride reduction method by using *Calix[6]rene* and *Calix[8]rene* as a stabilizing agents. The synthesized AuNPs were screened for cytotoxic, phytotoxic, antifungal and antibacterial activities. The fabricated AuNPs were characterized by UV–visible spectroscopy, atomic force microscopy (AFM) and FTIR spectroscopy. Antibacterial activities of the AuNPs were tested against *E. coli* and *S. aureus*. The *AuC6NPs* were found to be effective against the growth of gram positive bacteria and inhibited the growth of *S. aureus*. *AuC6NPs* interact with bacterial cell and damaged cell membrane. Roughness of the bacterial surface and membrane rupture can be clearly observed by AFM images. The AuNPs possess insignificant antifungal activity against *Aspergillus niger* and *Candida albicans*. Moreover, *AuC8NPs* have significant phytotoxicity and moderate cytotoxicity.

© 2019 Production and hosting by Elsevier B.V. on behalf of King Saud University. This is an open access article under the CC BY-NC-ND license (<http://creativecommons.org/licenses/by-nc-nd/4.0/>).

## 1. Background

Applications of nanoparticles (NPs) in different research areas such as nonmedicine (Chen et al., 2016; Swierczewska et al., 2016), water treatment (Donovan et al., 2016), cosmetics (Jiménez-Pérez et al., 2017) and agriculture (Servin and White, 2016) has risen considerably in recent past. NPs have

been used efficiently to develop various nano devices (Heerema and Dekker, 2016) and immunosensors for different biological, physical, pharmaceutical and biomedical applications (Ahmed et al., 2016; Anwar et al., 2018; Rao et al., 2017). Higher surface area to volume ratio and smaller size make them unique and active reagents for diverse applications. Functionalized gold nanoparticles are reported for their applications in a broad range due to their low toxicity, good stability and easy synthesis (Hornos Carneiro & Barbosa Jr, 2016). Functionalization of AuNPs with calixarenes opens new possibilities of applications. Calixarene is a macrocycle with unique three dimensional surfaces and is the subject of interest in biological domain since decades (Muneer et al., 2016; Nimse & Kim, 2013; Patil et al., 2016). Physical properties of NPs improve considerably by functionlaization with calixarene

\* Corresponding author.

E-mail address: [sadikhalid6@gmail.com](mailto:sadikhalid6@gmail.com) (S. Khalid).

Peer review under responsibility of King Saud University.



Production and hosting by Elsevier

due to its unique architecture. Hence, calixarene coalesce with the nanomaterials serve as a potential and attractive component in the field of nanotechnology.

In this study, we report functionalization of gold nanoparticles with calixarene in order to develop a new therapeutic agent. Calixarene stabilized nanomaterials have gained tremendous attraction and have been used in various fields such as catalysis (Panchal et al., 2017), sensors (Maity et al., 2014) and molecular recognition (Göde et al., 2017). Recently, Hennie et al carried out controlled fictionalization of nanoparticles with calixarene ligand (Valkenier et al., 2017). Giuseppe et al used calixarene-based nanoassembly as a potential vehicle for ophthalmic drug delivery (Granata et al., 2017). Nilesh et al successfully released doxorubicin into cancer cell while using silica-calix hybrid composites. Resent research suggests the shift of calixarene functionalized nanomaterial towards biomedical application.

Metals have been used as an antimicrobial agent since ancient time. Therefore a recent increase in the use of metal nanoparticles for development new therapeutic agents is noticed (Balogh et al., 2001; Chen et al., 2010; Luo et al., 2014). Comprehension studies on calixarene functionalized gold nanoparticles for antimicrobial effect along with cytotoxic effect are rarely reported (Kellici et al., 2016). The prime focus of current project is evaluation of the antimicrobial activities of AuNPs. The efficiency of synthesized AuNPs was investigated against gram positive and gram negative bacteria and fungi along with its cytotoxic and phototoxic effect. Calixarene coated AuNPs were synthesized by a simple and economical chemical reduction process. Antibacterial mechanism was checked at different doses of AuNPs against human pathogen bacteria: *E. coli*, and *S. aureus*. Change in cellular morphology of the bacteria was evaluated through AFM. *Aspergillus niger* and *Candida albicans* strains of fungi were used for antifungal activity and the zones of inhibition were calculated by the Agar well diffusion method.

## 2. Results and discussion

### 2.1. Characterization of synthesized AuNPs

UV-visible spectroscopy is one of the basic technique to determine the structure and optical properties of metallic nanoparticles because the position and shape of the absorption band is associated with the diameter and aspect ratio of metallic nanoparticles (Noguez, 2007). Colloidal AuNPs show a characteristic red color as the surface electron cloud vibrates and absorbs the electromagnetic radiation of a particular energy. The samples of AuNPs were prepared by a chemical approach and the variation in the UV-visible spectrum of the resultant sol was observed to analyze the size effect of metallic nanoparticles on surface Plasmon band (SPB).

UV-Visible spectra of the *AuC6NPs* showed SPB at 525 nm (Fig. 1A) and the SPB of *AuC8NPs* was observed at 540 nm (Fig. 1B), indicating reduction of  $\text{Au}^{3+}$  ions.

Atomic force microscopy (AFM) was executed to determine the particle size, and their size distribution of AuNPs (*AuC6NPs* and *AuC8NPs*). AFM analysis showed that fabricated AuNPs are spherical in shape however polydisperse. The analysis of histogram reveals that the *AuC6NPs* have size in range of 11–57 nm (Fig. 2A) whereas particle size of most of

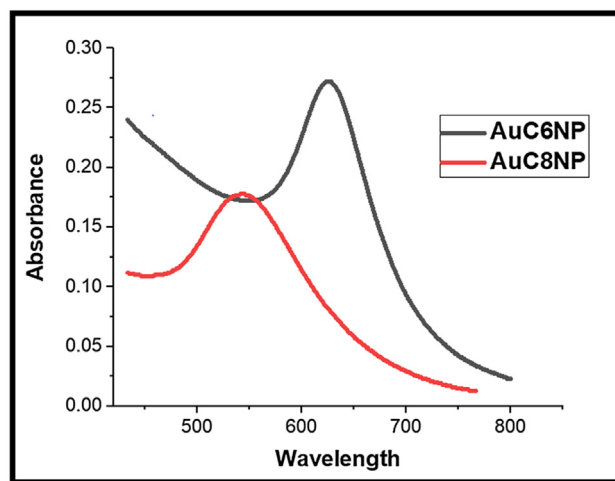


**Fig. 1** UV-visible spectrum for *AuC6NPs* and *AuC8NPs* respectively.

the NPs was found to be in the range of 31–34 nm. The sizes of *AuC8NPs* were in a range of 5–60 nm (Fig. 2B) with particles size of most of the NPs in the range of 41–44 nm. AFM results endorse the findings of UV-visible spectroscopy (Fig. 2A and B) (see Fig. 3).

The synthesized AuNPs (*AuC6NPs* and *AuC8NPs*) were subjected to FTIR analysis for understanding of the nature of interactions. The FTIR spectra of ligand *C6* and *C8* shows absorption band of medium intensity at  $3127\text{ cm}^{-1}$  for OH functionality (Gutsche, 2008). Absorption band at  $2960\text{ cm}^{-1}$  corresponds to CH asymmetric stretch. Aromatic ring bending vibration appears at  $1700\text{ cm}^{-1}$ , C–O stretching vibration appears at  $1482\text{ cm}^{-1}$  and tertiary alcohol vibration band is visible at  $1205\text{ cm}^{-1}$  in calixarene. After the formation of metallic nanoparticle peak at  $3127\text{ cm}^{-1}$  became more intense and broad that indicates the involvement of alcohol functionality in nanoparticles stabilization. On the other hand, shifting of band from  $1700\text{ cm}^{-1}$  to  $1798\text{ cm}^{-1}$  and  $1482\text{ cm}^{-1}$  to  $1408\text{ cm}^{-1}$  shows interaction of aromatic ring with nanoparticles.

### 2.2. Stability of gold nanoparticles

The stability of AuNPs is of prime concern when its different applications are sought. The stability of NPs is generally required over a wide pH range, in presence of electrolyte, and on temperature treatment. In this context, the effect presence of electrolyte on the stability of AuNPs was studied by addition of NaCl solution of varying the concentration (0.5 to 1000 mM) and AuNPs were found to be stable over a wide range of electrolyte concentration. On the same line, the pH effect on the stability of AuNPs is evaluated. *AuC6NPs* were found to be stable over whole pH range while *AuC8NPs* were stable in basic condition only (Fig. 4B).

### 2.3. Biological activities of synthesized AuNPs

The bactericidal effect of AuNPs (*AuC6NPs* and *AuC8NPs*) was evaluated against *E. coli* and *S. aureus*. The MIC value was calculated by monitoring the growth of *S. aureus* and *E. coli*. It is concluded that *AuC6NPs* have stronger effect on

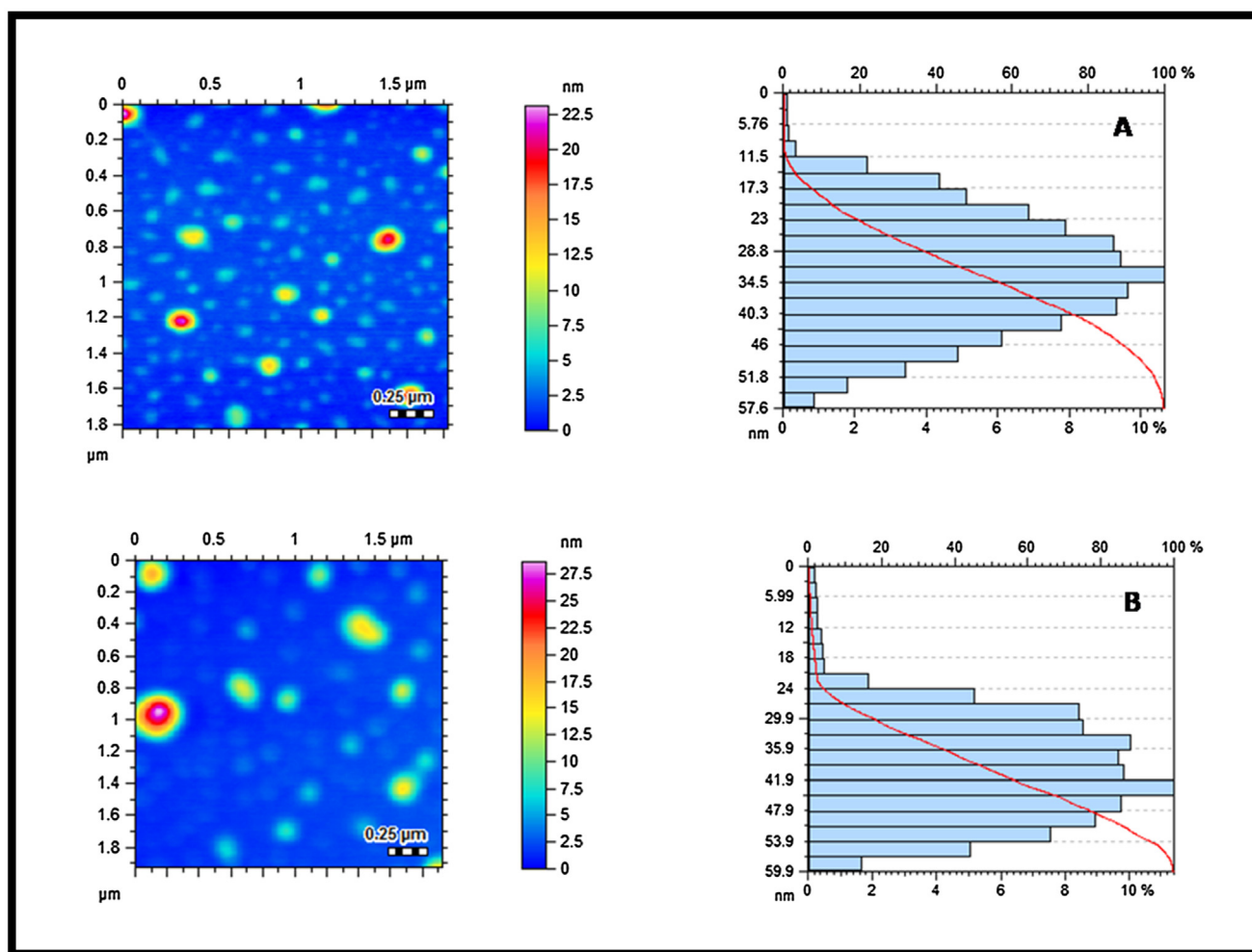


Fig. 2 Atomic force microscopy (AFM) analysis of AuNPs: topographical images and histograms (A) *AuC6NPs*; and (B) *AuC8NP*.

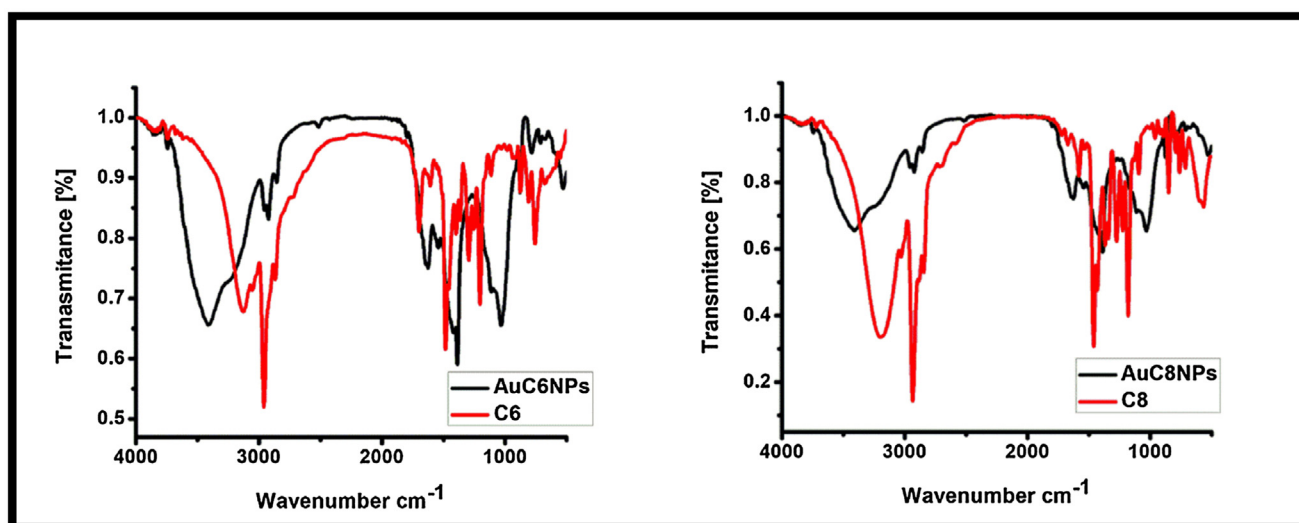


Fig. 3 FT-IR spectrum of gold nanoparticles (*AuC6NPs* and *AuC8NPs*) and ligand (*C6* and *C8*).

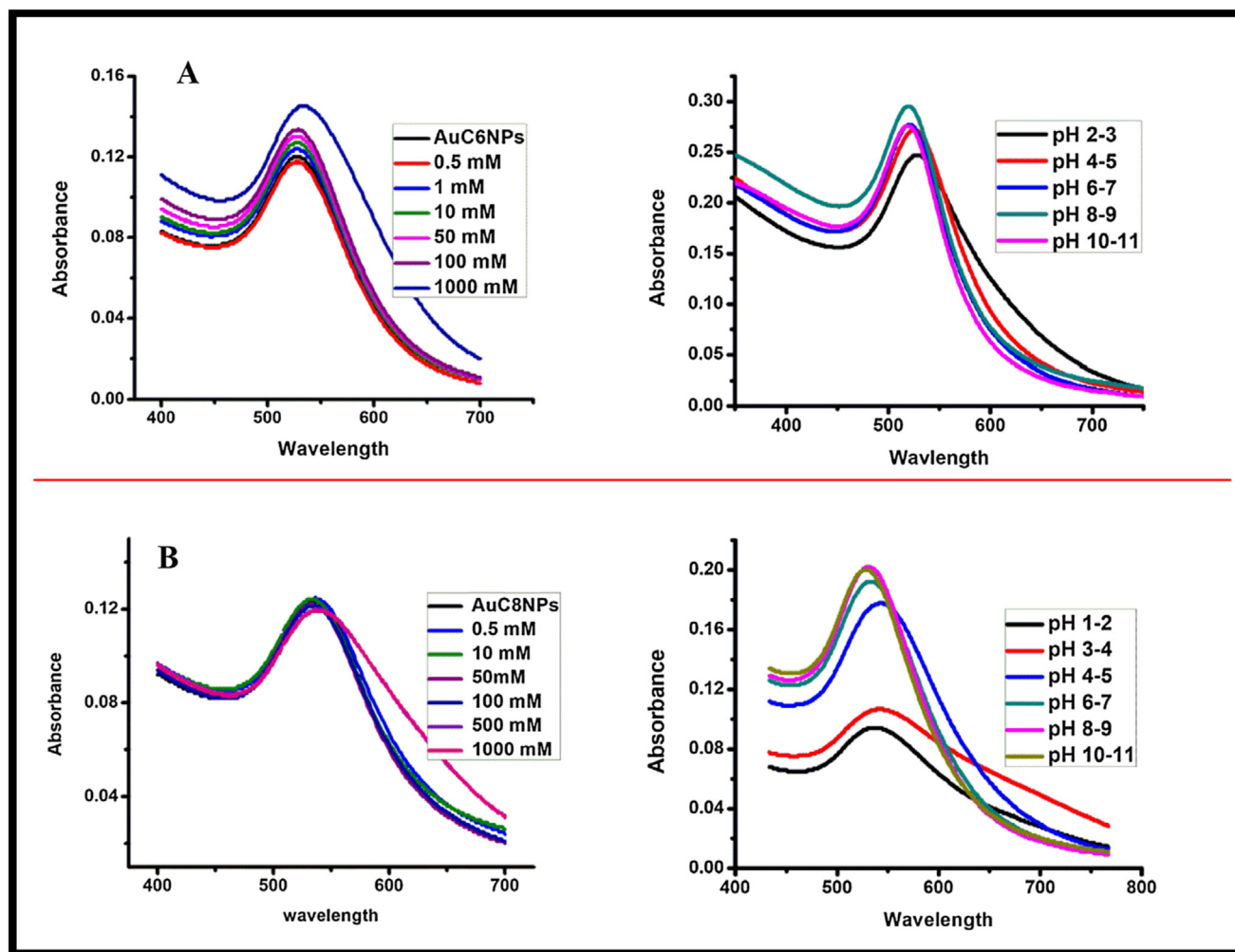


Fig. 4 Representing stability of gold nanoparticles (A) Effect of pH and salt on *AuC6NP* (B) effect of pH and salt on *AuC8NP*.

the growth of bacteria compared to *AuC8NPs*. Moreover, *AuC6NPs* inhibited the growth of both gram negative and gram positive bacteria.

The antibacterial effect of the AuNPs on different doses indicates that antibacterial action of AuNPs and ligands have dose dependency i.e. high antibacterial activity at high concentrations and *vice versa*. Maximum percent inhibition was observed at higher doses for both *S. aureus* and *E. coli*, Fig. 5. Having said that, *AuC6NPs* showed stronger effect against *S. aureus*, hence, are more potent compared to *AuC8NPs*. Maximum percent inhibition of *AuC6NPs* was calculated 90% for *S. aureus* and 60% for *E. coli* at 500  $\mu\text{g}/\text{mL}$ .

Subsequent changes in cell morphology of *E. coli* and *S. aureus* were examined by AFM, Figs. 6 and 7. The untreated bacterial strains of *E. coli* and *S. aureus* are compared with treated bacterial strains with C6 and *AuC6NPs*. Untreated *E. coli* and *S. aureus* were investigated and cultures exhibited cells with regular shapes and smooth membranes (Figs. 6A and 7A). This serves as a control for monitoring the changes after treatment. Cell degradation and membrane rupture were observed upon treatment with *AuC6NPs* and C6. *AuC6NPs* show extensive degradation unlike pure C6 ligand while, complete degradation of *S. aureus* cells is noticed after 24 h incuba-

tion leading to rough cell surface. Like behavior is observed for *E. coli* cells. Extensive membrane damage leads to the leakage of intercellular components and ultimately causing cell lysis. Morphological changes and cell rupture endorsed the binding and internalization of *AuC6NPs*. Hence, AFM images show clear evidence for antibacterial effect on *AuC6NPs*.

Antifungal activity was monitored by using two antifungal strains namely, *Aspergillus niger* and *Candida albicans*. None of the synthesized AuNPs showed significant activity against any strain of fungi. Thirty % inhibition of *AuC8NPs* against *Aspergillus niger* and twenty % against *Candida albicans* was observed. In case of *AuC6NPs* 25% inhibition was noticed against *Aspergillus niger* and 30% against *Candida albicans*. Comparison of both samples of gold nanoparticles against *Aspergillus niger* and against *Candida albicans* is demonstrated Fig. 8A. The results of phytotoxic analysis of AuNPs is depicted in Fig. 8B where *AuC8NPs* show 70% growth regulation while 45% growth regulation was observed for *AuC6NPs*. *AuC8NPs* have shown to be the more phytotoxic compared to *AuC6NPs*. Paraquat was used as a standard drug.

Brine shrimp viability bioassay was used to examine the potential toxicity of prepared AuNPs. Results of the toxicity evaluation against brine shrimp on both samples of gold

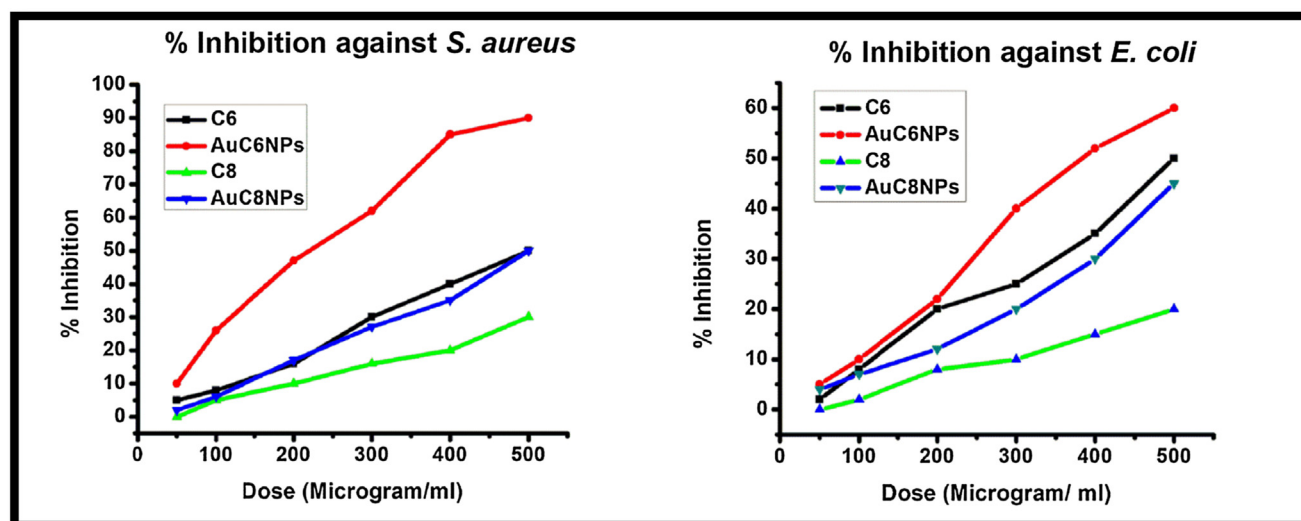


Fig. 5 % inhibition of gold nanoparticles (*AuC6NPs* and *AuC8NPs*) and ligand (*C6* and *C8*) against *E. coli* and *S. aureus*.

nanoparticles (*AuC6NPs* and *AuC8NPs*) showed the mortality at high concentration as shown in Table 1. Lethality was found to be directly proportional to the concentration. However, cytotoxic effects of gold nanoparticles toward shrimp's larvae can be linked to anticancer activity and can be used as a potential source of anticancer drugs.

Various AuNPs-based systems have been employed for antimicrobial applications. Recently Elisabetta de Alteriis and co-workers demonstrated in vitro antifungal activity of indolicidin-capped AuNPs (AuNPs-indolicidin) against *Candida albicans*. Similarly, Webster and co-workers reported mono and bimetallic NPs which are active against MDR *E. coli* (Webster & I cholula-Díaz, 2019). Above therapeutic agent is only active against gram negative strain whereas, our fabricated system is equally effective against both gram negative and positive bacteria. Major advantage of this work is, our synthesized NPs are economical, environmentally friendly and have shown competent results against both bacterial and fungal strains at the same time. Overall, our research offers a tremendous platform to design antimicrobial therapeutics in future studies. The present work suggests the nanoparticles may have potent anticancer activity. Further research is required to investigate the anticancer potential of the particles

#### 2.4. Conclusion

In this study, we report the successful preparation of gold nanoparticles by using *Calix[6]arene* and *Calix[8]arene* as a stabilizing agent. Synthesized gold nanoparticles were characterized by UV-vis spectroscopy, FT-IR and AFM. It is believed that hydroxyl group present in the ligand (*C6* and *C8*) has stabilized the gold ions into metallic nanoparticles. The synthesized *AuC6NPs* exhibited strong antibacterial activity against *S. aureus*. Furthermore, changes in cell structure and roughness on surface of the bacteria verify cell lysis. *AuC6NPs* killed bacteria with greater efficiency in comparison to ligand *C6*. Both samples of gold nanoparticles possess promising phytotoxicity and moderate cytotoxicity. Our synthesized gold nanoparticles may have commercial viability to

develop nanomedicine against different microbes and human pathogens. Taken together, cytotoxic and phytotoxic effects of gold nanoparticles can be linked with anticancer activity and hence, the synthesized nanoparticles could be alternative source of anticancer drugs.

### 3. Experimental section

#### 3.1. Materials

Analytical grade reagents such as hydrogen tetrachloroaurate (III) trihydrate ( $\text{HAuCl}_4 \cdot 3\text{H}_2\text{O}$ ) 99.995%, sodium borohydride ( $\text{NaBH}_4$ ) 98%, *calix[6]arene* 97% and *calix[8]arene* 90% were purchased from Sigma Aldrich. The solutions were prepared in deionized water. For antibacterial activity *E. coli* and *S. aureus* bacterial strains were used whereas antifungal activities were carried out by using *Aspergillus niger* and *Candida albicans* fungal strains.

#### 3.2. Synthesis of gold nanoparticles

The AuNPs were synthesized by using sodium borohydride as a reducing agent. Initially the solutions of *calix[6]arene* (*C6*) and *calix[8]arene* (*C8*) were prepared in DMF which were further diluted in deionized water to prepare 0.1 mM solution. Two samples of AuNPs (*AuC6NPs* and *AuC8NPs*) were synthesized by adding 5 mL *C6* to sample 1 and 3 mL *C8* to sample 2 in tetrachloroaurate (III) trihydrate solution (0.1 mM, 30 mL). The samples were reduced by drop wise addition of sodium borohydride (4 mM). Pink color was obtained immediately after adding  $\text{NaBH}_4$ , the mixture was stirred till wine red is obtained.

#### 3.3. Methodology of antifungal activity

The Agar tube dilution Method was used to determine antifungal activity (Atta-ur-Rahman & Abbas, 1991) and Amphotericin B was used as a standard. All the samples and standard were dissolved in sterilized distilled water/

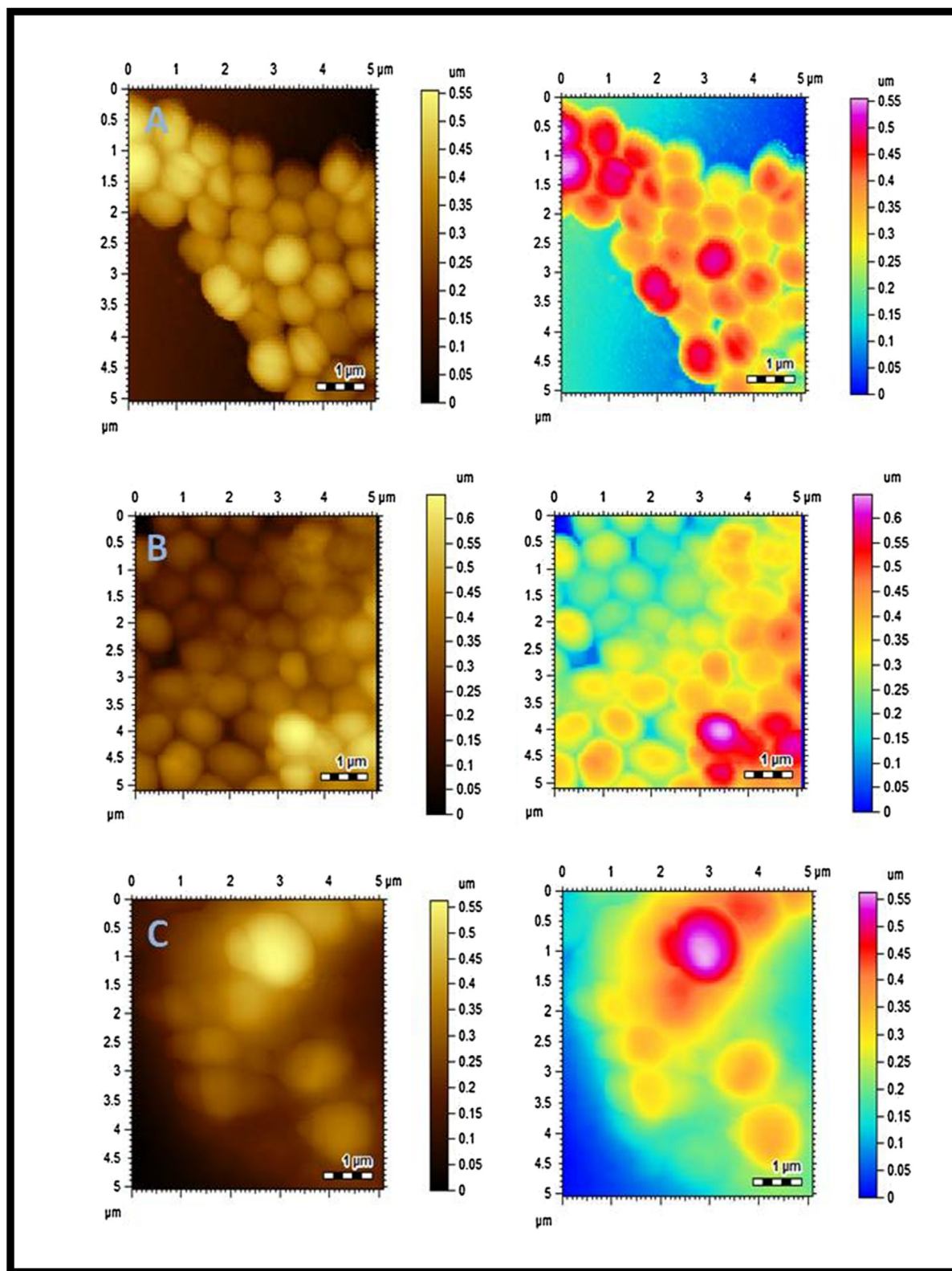


**Fig. 6** AFM images of *S. aureus*. (A) Control (B) C6 treated *S. aureus* (C) AuC6NPs treated *S. aureus*.

DMSO (24 mg/mL). Samples with various concentrations (50–400  $\mu\text{g}/\text{ml}$ ) were placed in test tube containing sterile Sabouraud's Dextrose agar medium and were inoculated in

slanting position at room temperature for overnight. After inoculation fungal cultures the samples were left to incubate for 7 days at 29 °C. While, Growth inhibition was calculated

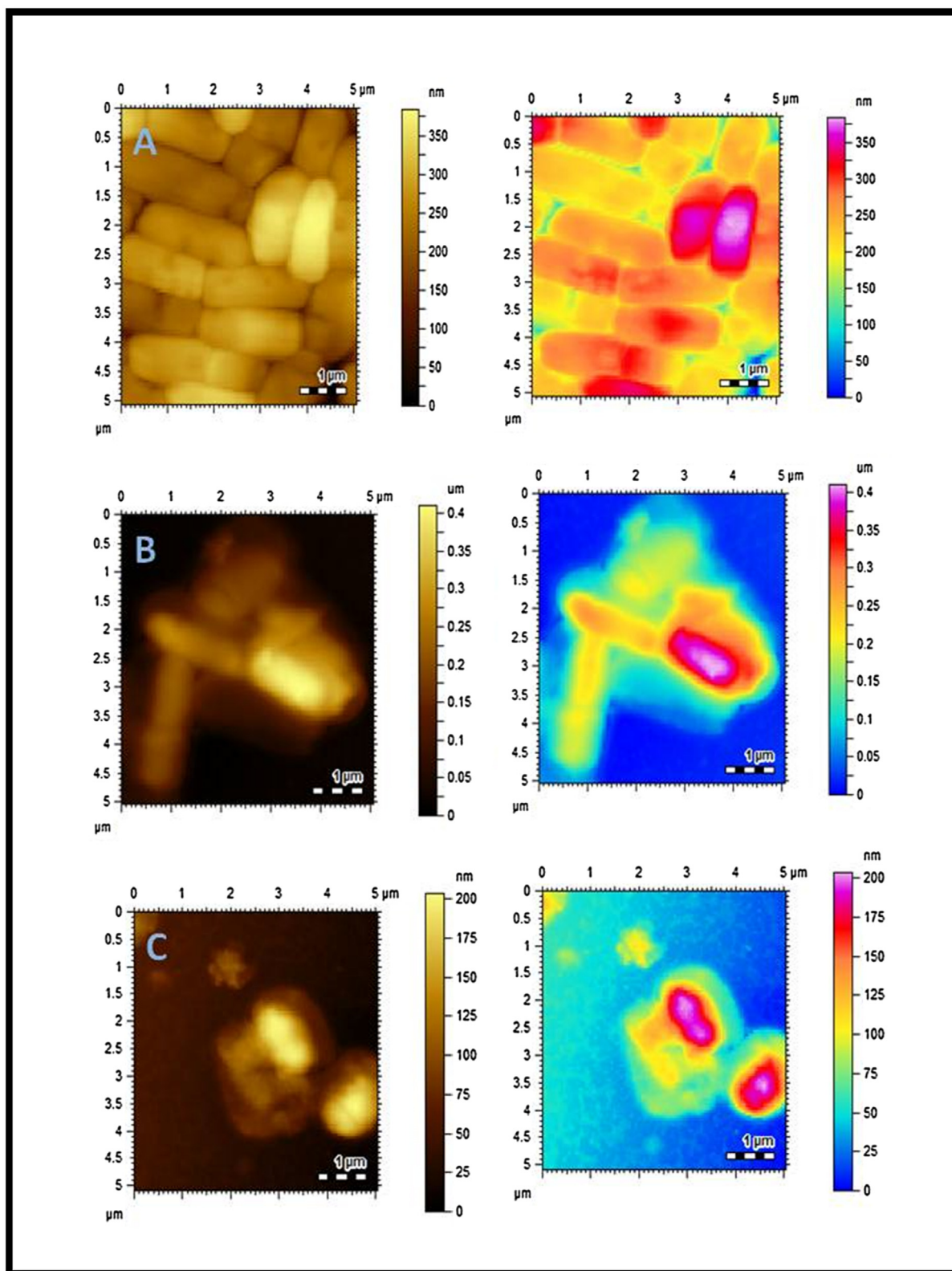


Fig. 7 AFM images of *E. coli*. (A) Control (B) C6 treated *E. coli* (C) AuC6NPs treated *E. coli*.

against reference to the negative control by applying following formula:

$\% \text{ inhibition of fungal growth} = 100 - \frac{\text{linear growth and test (mm)}}{\text{linear growth in control (mm)}} \times 100$

### 3.4. Methodology of antibacterial activity

Bacterial cultures were grown in nutrient agar medium at the concentration of  $10^5$  cells/mL. Later, a hole of 60 mm was

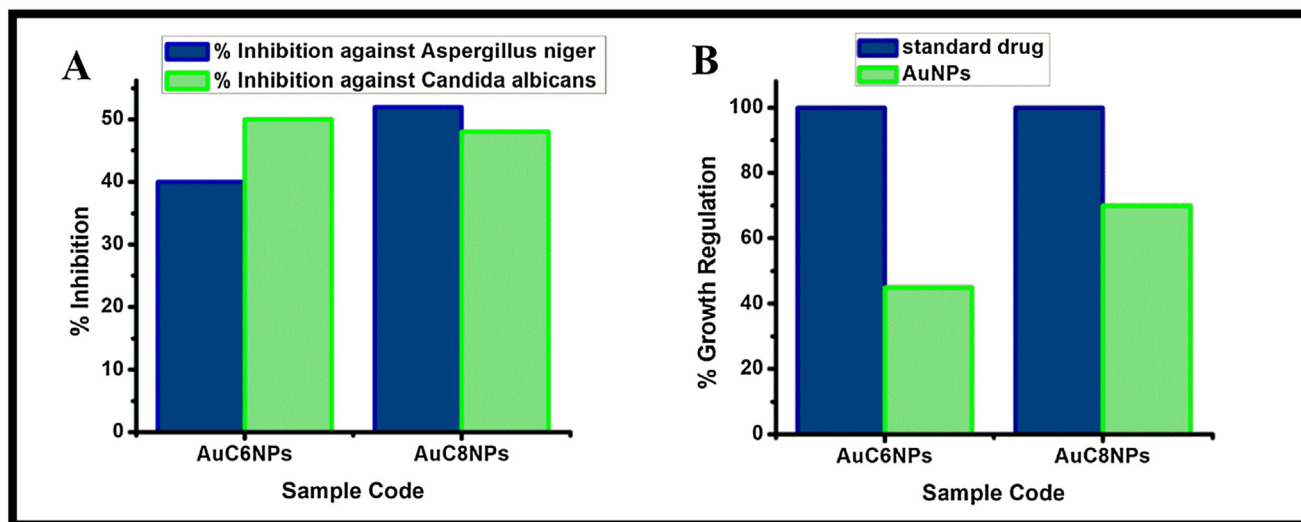


Fig. 8 Antifungal and phytotoxic analysis of AuNPs.

**Table 1** Brine shrimp lethality bioassay analysis of *AuC6NPs* and *AuC8NPs* gold nanoparticles.

Sample code	Dose ( $\mu\text{g/ml}$ )	No. of shrimps	No. of survivors	LD <sub>50</sub> of nanoparticle ( $\mu\text{g/ml}$ )	LD <sub>50</sub> of Std. Drug ( $\mu\text{g/ml}$ )
<i>AuC8NPs</i>	0.0129		25		
	0.129	30	24	66.7184	7.2539
	1.29		20		
<i>AuC6NPs</i>	0.013		23		
	0.13	30	22	21.37	20.5459
	1.3		18		

Paraquat is used as a standard drug.

Incubation conditions =  $28 \pm 1^\circ\text{C}$ .

made in each plate by using a borer, Different concentrations ranging from 10 to 500  $\mu\text{g/ml}$  of Ceftriaxone, and AuNPs were inserted in each hole simultaneously to evaluate the efficiency of methodology. However, 500  $\mu\text{g mL}^{-1}$  stock solutions of Ceftriaxone, and AuNPs were used to avoid nonspecific merged zones of inhibition. The plates were incubated at  $37^\circ\text{C} \pm 1$  for 24 h. After 24 h incubation, zone of inhibition was calculated at millimeter scale. Afterwards Minimal Inhibitory Concentration (MIC) of gold nanoparticles was calculated against each bacterial strain, for *E. coli* = Ceftriaxone MIC was calculated 10  $\mu\text{g/ml}$  and for *S. aureus* was calculated 20  $\mu\text{g/ml}$ . Two bacterial strains *S. aureus ATCC 9144* and *E. coli ATCC 10536* were used to evaluate antibacterial activity of samples.

### 3.5. Brine shrimp lethality assay

Cytotoxic activity of synthesized AuNPs was determined by brine shrimp lethality assay. Sample was prepared by taking 2 mL of AuNPs solutions in a vial and 5, 50, 500  $\mu\text{L}$  of prepared solution of AuNPs was transferred to other three vials. Brine shrimp (*Artemia saline*) eggs were hatched in artificial sea water (prepared by dissolving 38 g/L sea salt in water) and were incubated for 48 h at  $37^\circ\text{C}$ . After 2 days nauplii were transferred with Pasteur pipette in the vials containing 2 mL of sample. Teen

larvae were transferred to each vials and sea water was added to make volume up to 5 mL. A vial containing 50  $\mu\text{L}$  DMSO instead of sample was used as control. After 24 h of incubation the number of survived shrimps were counted and recorded in each vial. Etoposide was used as a positive control. Final data was analyzed with Finney computer program to determine the LD<sub>50</sub> values with 95% confidence level.

### 3.6. The Lemna bioassay

Phytotoxic activity of AuNPs was determined by using the modified protocol of Lemna minor. Different constituents were mixed in 1000 mL distilled water to prepare medium and the pH (6.0 to 7.0) of the medium was adjusted by KOH solution. The E-medium was prepared by adding 100 mL of stock solution into 900 mL of distilled water. Three flasks were inoculated with 10, 100, and 1000  $\mu\text{L}$  from the stock solution of AuNPs for 10, 100, and 1000  $\mu\text{g/ml}$  respectively. The solution was left to evaporate under sterile conditions for overnight. 20 mL of E-medium was added to each flask containing a rosette of three fronds of Lemna minor was added. All flasks were plugged with cotton and placed in the growth cabinet for 7 days. The number of fronds per flask was counted and their growth regulation was calculated with the reference to the negative control.

### 3.7. Characterization technique

UV-visible spectroscopy (Thermo Scientific Evolution 300 spectrophotometer) and FT-IR (Bruker Victor 22 spectrophotometer) were employed for analysis.

### 3.8. Analysis of cellular morphology

Change in morphology on bacterial surface was monitored by Agilent 5500 Atomic Force Microscopy (AFM), (Arizona USA). Initially mica slides were prepared by adding 10 mL polylysine. Treated and untreated *S. aureus*, *E. coli* cultures were placed on already prepared mica slides and air-dried. These air-dried slides were then subjected for AFM analysis. The variations in the morphology of treated and untreated samples were evaluated. The images were acquired in tapping mode.

### 3.9. Abbreviations

**NP:** nanoparticles **AuNP:** gold nanoparticles **AFM:** atomic force microscopy **SPB:** surface Plasmon band **C6:** calix[6]arene **C8:** calix[8]arene

## 4. Declarations

### Authors contributions

SK Synthesized and characterized the nanoparticles and wrote the manuscript. SP and SA performed biological work. MRS designed project and supervised studies. SR interpreted biological analyses. MIM corrected and finalized the manuscript. All authors read and approved the final manuscript.

### Acknowledgement

All authors are thankful to the ICCBS, University of Karachi for instrumental support.

### Competing interest

The authors declare that they have no competing interests.

## References

- Ahmed, A., Khan, A.K., Anwar, A., Ali, S.A., Shah, M.R., 2016. Biofilm inhibitory effect of chlorhexidine conjugated gold nanoparticles against *Klebsiella pneumoniae*. *Microb. Pathog.* 98, 50–56.
- Anwar, A., Khalid, S., Perveen, S., Ahmed, S., Siddiqui, R., Khan, N. A., Shah, M.R., 2018. Synthesis of 4-(dimethylamino) pyridine propylthioacetate coated gold nanoparticles and their antibacterial and photophysical activity. *J. Nanobiotechnol.* 16 (1), 6.
- Balogh, L., Swanson, D.R., Tomalia, D.A., Hagnauer, G.L., McManus, A.T., 2001. Dendrimer-silver complexes and nanocomposites as antimicrobial agents. *Nano Lett.* 1 (1), 18–21.
- Chen, G., Roy, I., Yang, C., Prasad, P.N., 2016. Nanochemistry and nanomedicine for nanoparticle-based diagnostics and therapy. *Chem. Rev.* 116 (5), 2826–2885.
- Chen, W.-Y., Lin, J.-Y., Chen, W.-J., Luo, L., Wei-Guang Diau, E., Chen, Y.-C., 2010. Functional gold nanoclusters as antimicrobial agents for antibiotic-resistant bacteria. *Nanomedicine* 5 (5), 755–764.
- Donovan, A.R., Adams, C.D., Ma, Y., Stephan, C., Eichholz, T., Shi, H., 2016. Single particle ICP-MS characterization of titanium dioxide, silver, and gold nanoparticles during drinking water treatment. *Chemosphere* 144, 148–153.
- Göde, C., Yola, M.L., Yılmaz, A., Atar, N., Wang, S., 2017. A novel electrochemical sensor based on calixarene functionalized reduced graphene oxide: application to simultaneous determination of Fe (III), Cd (II) and Pb (II) ions. *J. Colloid Interface Sci.* 508, 525–531.
- Granata, G., Paterniti, I., Geraci, C., Cunsolo, F., Esposito, E., Cordaro, M., Consoli, G.M., 2017. Potential eye drop based on a calix [4] arene nanoassembly for curcumin delivery: enhanced drug solubility, stability, and anti-inflammatory effect. *Mol. Pharm.* 14 (5), 1610–1622.
- Gutsche, C.D., 2008. Calixarenes: an introduction. Royal Society of Chemistry.
- Heerema, S.J., Dekker, C., 2016. Graphene nanodevices for DNA sequencing. *Nat. Nanotechnol.* 11 (2), 127–136.
- Hornos Carneiro, M.F., Barbosa Jr, F., 2016. Gold nanoparticles: a critical review of therapeutic applications and toxicological aspects. *J. Toxicol. Environ. Health B* 19 (3–4), 129–148.
- Jiménez-Pérez, Z.E., Singh, P., Kim, Y.-J., Mathiyalagan, R., Kim, D.-H., Lee, M.H., Yang, D.C., 2017. Applications of Panax ginseng leaves-mediated gold nanoparticles in cosmetics relation to antioxidant, moisture retention, and whitening effect on B16BL6 cells. *J. Ginseng Res.*
- Kellici, S., Acord, J., Vaughn, A., Power, N.P., Morgan, D.J., Heil, T., Lampronti, G.I., 2016. Calixarene assisted rapid synthesis of silver-graphene nanocomposites with enhanced antibacterial activity. *ACS Appl. Mater. Interfaces* 8 (29), 19038–19046.
- Luo, Z., Zheng, K., Xie, J., 2014. Engineering ultrasmall water-soluble gold and silver nanoclusters for biomedical applications. *Chem. Commun.* 50 (40), 5143–5155.
- Maity, D., Gupta, R., Gunupuru, R., Srivastava, D.N., Paul, P., 2014. Calix [4] arene functionalized gold nanoparticles: application in colorimetric and electrochemical sensing of cobalt ion in organic and aqueous medium. *Sens. Actuat. B* 191, 757–764.
- Muneer, S., Memon, S., Panhwar, Q.K., Khushik, F., Khokhar, T.S., Noor, A.A., 2016. Synthesis and antimicrobial activity of p-tetranitrocalix [4] arene derivative. *Polycyclic Aromat. Compd.* 36 (4), 554–563.
- Nimse, S.B., Kim, T., 2013. Biological applications of functionalized calixarenes. *Chem. Soc. Rev.* 42 (1), 366–386.
- Noguez, C., 2007. Surface plasmons on metal nanoparticles: the influence of shape and physical environment. *J. Phys. Chem. C* 111 (10), 3806–3819.
- Panchal, M., Kongor, A., Mehta, V., Vora, M., Bhatt, K., Jain, V., 2017. Heck-type olefination and Suzuki coupling reactions using highly efficient oxacalix [4] arene wrapped nanopalladium catalyst. *J. Saudi Chem. Soc.*
- Patil, S.V., Athare, S.V., Jagtap, A., Kodam, K.M., Gejji, S.P., Malkhede, D.D., 2016. Encapsulation of rhodamine-6G within p-sulfonatocalix [n] arenes: NMR, photophysical behaviour and biological activities. *RSC Adv.* 6 (111), 110206–110220.
- Rao, K., Imran, M., Jabri, T., Ali, I., Perveen, S., Ahmed, S., Shah, M. R., 2017. Gum tragacanth stabilized green gold nanoparticles as cargos for Naringin loading: a morphological investigation through AFM. *Carbohydr. Polym.* 174, 243–252.
- Servin, A.D., White, J.C., 2016. Nanotechnology in agriculture: next steps for understanding engineered nanoparticle exposure and risk. *NanoImpact* 1, 9–12.
- Swierczewska, M., Han, H., Kim, K., Park, J., Lee, S., 2016. Polysaccharide-based nanoparticles for theranostic nanomedicine. *Adv. Drug Deliv. Rev.* 99, 70–84.
- Valkenier, H., Malyskyi, V., Blond, P., Retout, M., Mattiuzzi, A., Goole, J., Bruylants, G., 2017. Controlled functionalization of gold nanoparticles with mixtures of calix [4] arenes revealed by infrared spectroscopy. *Langmuir* 33 (33), 8253–8259.